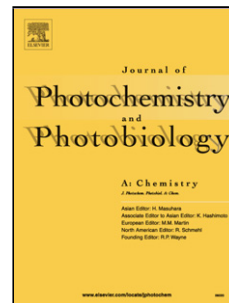


# Journal Pre-proof

Fluorescent chemical sensor based on double  $N_2O_2$  cavities for continuous recognition of  $Cu^{2+}$  and  $Al^{3+}$

Ruo-Nan Bian, Ji-Fa Wang, Ya-Juan Li, Yang Zhang, Wen-Kui Dong



PII: S1010-6030(20)30627-4

DOI: <https://doi.org/10.1016/j.jphotochem.2020.112829>

Reference: JPC 112829

To appear in: *Journal of Photochemistry & Photobiology, A: Chemistry*

Received Date: 15 June 2020

Revised Date: 27 July 2020

Accepted Date: 3 August 2020

Please cite this article as: Bian R-Nan, Wang J-Fa, Li Y-Juan, Zhang Y, Dong W-Kui, Fluorescent chemical sensor based on double  $N_2O_2$  cavities for continuous recognition of  $Cu^{2+}$  and  $Al^{3+}$ , *Journal of Photochemistry and Photobiology, A: Chemistry* (2020), doi: <https://doi.org/10.1016/j.jphotochem.2020.112829>

This is a PDF file of an article that has undergone enhancements after acceptance, such as the addition of a cover page and metadata, and formatting for readability, but it is not yet the definitive version of record. This version will undergo additional copyediting, typesetting and review before it is published in its final form, but we are providing this version to give early visibility of the article. Please note that, during the production process, errors may be discovered which could affect the content, and all legal disclaimers that apply to the journal pertain.

© 2020 Published by Elsevier.

## Fluorescent chemical sensor based on double $\text{N}_2\text{O}_2$ cavities for continuous recognition of $\text{Cu}^{2+}$ and $\text{Al}^{3+}$

Ruo-Nan Bian, Ji-Fa Wang, Ya-Juan Li, Yang Zhang, Wen-Kui Dong\*

School of Chemical and Biological Engineering, Lanzhou Jiaotong University,  
Lanzhou, Gansu 730070, China

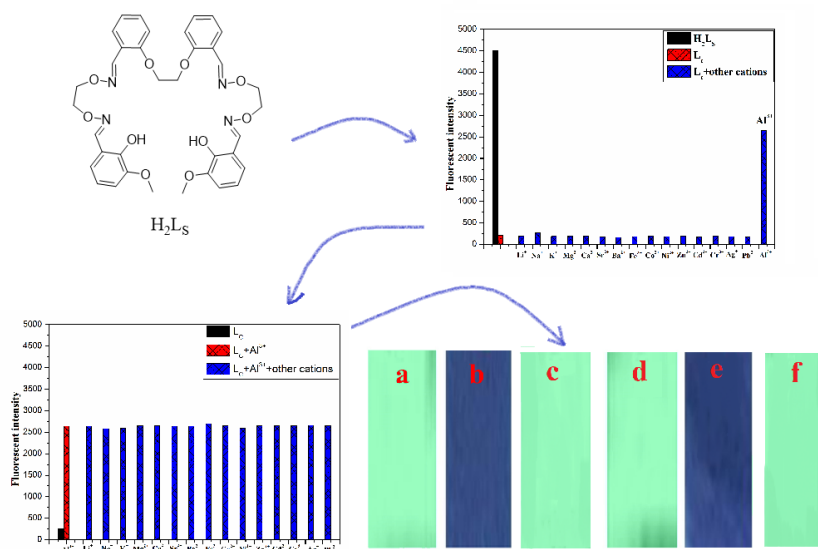
\*Corresponding author.

E-mail addresses: dongwk@126.com (W.-K. Dong).

### Graphical Abstract

A new bis(salamo)-based chemical sensor  $\text{H}_2\text{Ls}$  for continuous recognition of  $\text{Cu}^{2+}$ ,  $\text{Al}^{3+}$  was synthesized. The chemical sensor  $\text{H}_2\text{Ls}$  can detect  $\text{Cu}^{2+}$  by the phenomenon of fluorescence quenching, and a test strip loaded with the sensor is used to quickly and accurately identify  $\text{Cu}^{2+}$ . Chemical sensor  $\text{H}_2\text{Ls}$  not only can detect  $\text{Cu}^{2+}$  in environmental water sample, but also continuously recognize  $\text{Al}^{3+}$ , and realize the interference-free identification effect of other trivalent metal ions on  $\text{Al}^{3+}$ .

Continuously recognize  $\text{Cu}^{2+}$ ,  $\text{Al}^{3+}$  :



## Highlights

- A new bis(salamo)-based chemical sensor **H<sub>2</sub>L<sub>5</sub>** for continuous recognition of  $\text{Cu}^{2+}$ ,  $\text{Al}^{3+}$  was synthesized.
- The chemical sensor **H<sub>2</sub>L<sub>5</sub>** can detect  $\text{Cu}^{2+}$  by the phenomenon of fluorescence quenching, and a test strip loaded with the sensor is used to quickly and accurately identify  $\text{Cu}^{2+}$ .
- Chemical sensor **H<sub>2</sub>L<sub>5</sub>** not only can detect  $\text{Cu}^{2+}$  in environmental water sample, but also continuously recognize  $\text{Al}^{3+}$ , and realize the interference-free identification effect of other trivalent metal ions on  $\text{Al}^{3+}$ .

## Abstract

A fluorescent chemical sensor based on a bis(salamo)-like tetraoxime **H<sub>2</sub>L<sub>5</sub>** was designed and synthesized. The chemical sensor uses double  $\text{N}_2\text{O}_2$  cavities as sensing elements, which can be combined with specific metal ions to achieve ion recognition. The chemical sensor can detect  $\text{Cu}^{2+}$  by the phenomenon of fluorescence quenching, and a test strip loaded with the sensor is used to quickly and accurately identify  $\text{Cu}^{2+}$ . Besides, the chemical sensor also can continuously recognize  $\text{Al}^{3+}$  in the system and

realize the interference-free identification effect of other trivalent metal ions on  $\text{Al}^{3+}$ . Through  $^1\text{H}$  NMR, mass spectrometry, infrared spectroscopy, and other experiments, the identification mechanism of the fluorescent chemical sensor was verified. The numerical values of LOD and  $K_a$  were calculated by the corresponding titration data and Benesi-Hildebrand formula.

*Keywords:* bis(salamo)-like tetraoxime; fluorescent chemical sensor;  $\text{Cu}^{2+}$  ion;  $\text{Al}^{3+}$  ion; test paper strip

## 1. Introduction

At present, water scarcity and metal pollution are two of the major problems of our water resources [1-7]. Contamination of water resources by metals and other harmful ions not only seriously affect the ecological environment but also directly pollute the soil, resulting in metal pollution of agricultural products, threatening human health [8-13]. Nowadays, many agricultural products have been found to contain metal elements, so the development of a fast, accurate, and efficient method to detect metal ions in complex water samples is the focus and hotspot of environmental science and biomedical research [14-18]. Fluorescence sensor molecules are widely used in ion detection because of their facile synthesis, high sensitivity and selectivity, fast response, and high interference resistance [19].

Salamo-like compounds have higher stability compared to salen-like compounds, and the symmetrical double salamo-like compound has excellent flexibility and several different cavities with high selectivity and metal ions [20-25]. Therefore, the balanced bis(salamo)-like compounds can interact with many metal ions to form metal complexes, which have considerable potential in ion recognition, supramolecular construction, and biological applications. Salamo-like compounds are derivatives of salen-like compounds by modifying the  $-\text{C}=\text{N}-$  group in salen compounds to the  $-\text{C}=\text{N}-\text{O}-$  group, which introduces an electronegative O-atom, making them  $10^4$  times more stable than salen compounds [26-29]. The design and

introduction of different functional groups to modify the end groups can indirectly regulate the solubility of these ligands in aqueous systems, thereby expanding the range of detection of these compounds as fluorescent chemical sensors for different ions in the environment [30-35]. Copper is one of the trace elements essential for life in plants and animals and plays a critical role in the life process. Many of the active sites of metallizes and metalloproteins contain dinuclear copper(II) structural units [36-40]. Besides, copper has a large number of coordination points and excellent coordination properties and can form copper(II) complexes with most ligands, making the study of copper(II) coordination more convenient. The application of copper(II) compounds in catalytic and optoelectronic materials is gradually becoming a research focus [41-43]. The stable order of complexes generated from  $Mn^{2+}$  to  $Zn^{2+}$  divalent metals with ligands containing N coordination atoms can be observed in the following order:  $Mn^{2+} < Fe^{2+} < Co^{2+} < Ni^{2+} < Cu^{2+} > Zn^{2+}$ , the sequence called the Irving-Williams sequence, which roughly corresponds to the variation of the weak-field CFSE [44-45]. Based on the Irving-Williams sequence, the copper complexes are more stable in comparison to those of other same period divalent metal ions.

**H<sub>2</sub>Ls** was found to recognize copper(II) ions and to recognize aluminum(III) ions directionally after the formation of copper(II) complexes. Excess aluminum(III) ion in the human body is not suitable for skeletal development and can also affect intelligence, so the complex  $[(Ls + 2Cu^{2+})NO_3^-]^+$  (**Lc**) has the necessary implications and developmental prospects for the detection of aluminum(III) ions in organisms.

The  $Cu^{2+}$  ions were first detected by using the bis(salamo)-like chemical sensor **H<sub>2</sub>Ls**. The experimental results showed that sensor **H<sub>2</sub>Ls** can detect  $Cu^{2+}$  in aqueous solution by the fluorescence quenching phenomenon. The advantages of the sensor **H<sub>2</sub>Ls** for detection of  $Cu^{2+}$  include a low detection limit, high coordination constant, wide pH range and fast response time. In addition, a test paper equipped with the sensor **H<sub>2</sub>Ls** was prepared, which can be used to detect the presence of  $Cu^{2+}$  easily, quickly, accurately and qualitatively in aqueous solution. Hence, sensor **H<sub>2</sub>Ls** has potential applications for  $Cu^{2+}$  detection in real life. Besides, the sensor **H<sub>2</sub>Ls** can continuously identify  $Al^{3+}$  in the system and achieves interference-free identification

of  $\text{Al}^{3+}$  by other trivalent metal ions. Finally, test paper strip experiments were done, and the results showed that this fluorescent chemical sensor could be applied to the test paper to detect specific ions quickly.

## 2. Experimental section

### 2.1 Experimental methods and instruments

All chemicals and solvents were analytical grade reagents from Tianjin Chemical Reagent Factory and were used without further purification. Elemental analyses were obtained on a GmbH VarioEL V3.00 automated elemental analysis instrument. Melting points were obtained by a microscopic melting point apparatus made in Beijing Taiké Instrument Limited Company and were uncorrected.  $^1\text{H}$  NMR spectra were measured by German Bruker AVANCE DRX-400 spectrometer. Fluorescence spectra were recorded on the Hitachi F-7000 spectrometers. ESI-MS spectra were measured on the Bruker Daltonics Esquire 6000 mass spectrometer. All pH measurements were made with a PHS-45 digital pH meter.

### 2.2 Synthesis and characterization of $\text{H}_2\text{Ls}$

The bis(salamo)-like tetraoxime  $\text{H}_2\text{Ls}$  was designed and synthesized based on previously reported research methods and test routes in this laboratory. [46,47]

#### Scheme 1. Synthetic route to sensor $\text{H}_2\text{Ls}$

2,2'-(Ethylenedioxy)bis(benzaldehyde)(**1**) was synthesized according to a literature procedure [48].

2-[*O*-(1-Ethoxyamide)]oxime-6-methoxyphenol(**2**) was prepared according to a previously reported method [49-52]. Weighing 1,2-bis(aminoxy)ethane(**d**) 414.45 mg (4.5 mmol) in ethanol (20 mL), another 684.67 mg (4.5 mmol) of 3-methoxysalicylaldehyde(**c**) was dissolved in ethanol (20 mL). An ethanol solution of 3-methoxysalicylaldehyde(**c**) was added drop by drop to an ethanol solution of 1,2-bis(aminoxy)ethane(**d**) in a water bath at  $55^\circ\text{C}$ , with a controlled drop

acceleration of about 10 s a drop and continuous reaction for 6 h to obtain light yellow ethanol solution. Decompression distillation removes excess solvent and concentrates the reaction solution to about 5 mL. The concentrated solution is a bright yellow oily liquid, further purified by column chromatography to obtain white solid 748.44 mg, yield: 73.51%; m.p.: 95.5-96.5°C. Anal. Calcd. for C<sub>10</sub>H<sub>14</sub>N<sub>2</sub>O<sub>4</sub>: C, 53.09; H, 6.24; N, 12.38. Found: C, 53.32; H, 6.20; N, 12.16. <sup>1</sup>H NMR (500 MHz, CDCl<sub>3</sub>) δ 3.92 (s, 3H), 3.96 (t, *J* = 4.5 Hz, 2H), 4.38 (t, *J* = 4.5 Hz, 2H), 5.50 (brs, 2H), 6.82 (dd, *J* = 7.8, 1.6 Hz, 1H), 6.87 (t, *J* = 7.8 Hz, 1H), 6.90 (dd, *J* = 7.8, 1.6 Hz, 1H), 8.24 (s, 1H), 9.88 (s, 1H).

An ethanol solution (10 mL) of 2,2'-(ethylenedioxy)bis(benzaldehyde)(**1**) (270.22 mg, 1.0 mmol) was added drop by drop to an ethanol solution (20 mL) of 2-[*O*-(1-ethoxyamide)]oxime-6-methoxyphenol(**2**) (453.08 mg, 2.0 mmol) in a water bath at 55°C, and the reaction continued for 4h. A large amount of white precipitation occurred in the solution. At the end of the reaction, the distillation was decompressed to remove the excess solvent, filtered and dried. White solid: 517.29 mg. Yield: 75.32%. m.p.: 124.6-126.4°C. Anal. calcd. For C<sub>36</sub>H<sub>38</sub>N<sub>4</sub>O<sub>10</sub>: C, 62.97; H, 5.58; N, 8.16. Found: C, 63.15; H, 5.49; N, 8.09. <sup>1</sup>H NMR (500 MHz, CDCl<sub>3</sub>) δ 9.82 (s, 2H), 8.51 (s, 2H), 8.23 (s, 2H), 7.79 (d, *J* = 7.7 Hz, 2H), 7.34 (t, *J* = 8.7 Hz, 2H), 6.97 (t, *J* = 7.5 Hz, 2H), 6.93 (d, *J* = 8.4 Hz, 2H), 6.90 (d, *J* = 6.8 Hz, 2H), 6.84 (t, *J* = 7.8 Hz, 2H), 6.79 (dd, *J* = 7.7, 1.5 Hz, 2H), 4.47-4.45 (m, 4H), 4.45-4.43 (m, 4H), 4.35 (s, 4H), 3.89 (s, 6H) ( **Figure S1**).

## 2.3 Experimental methods

### 2.3.1 Solution preparation

The samples used in the fluorescence spectroscopy of this experiment, including the bis(salamo)-like tetraoxime chemical sensor **H<sub>2</sub>LS** and the metal ions, were configured with a solution. The probe molecule is [**H<sub>2</sub>LS**] = 1 × 10<sup>-3</sup> mol/L. The metal ion solutions are derived from their metal nitrates. Metal ions [**M<sup>n+</sup>**] = 1 × 10<sup>-2</sup> mol/L (Li<sup>+</sup>, Na<sup>+</sup>, K<sup>+</sup>, Mg<sup>2+</sup>, Ca<sup>2+</sup>, Sr<sup>2+</sup>, Ba<sup>2+</sup>, Cr<sup>3+</sup>, Fe<sup>3+</sup>, Co<sup>2+</sup>, Ni<sup>2+</sup>, Cu<sup>2+</sup>, Zn<sup>2+</sup>, Cd<sup>2+</sup>, Ag<sup>+</sup> and Al<sup>3+</sup>).

### 2.3.2 Fluorescence spectroscopy experiment

The fluorescence spectroscopy experiments were performed with a reserve solution of chemical sensor **H<sub>2</sub>LS** ( $V_{\text{DMF}}: V_{\text{Water}} = 9:1$ ,  $c = 1 \times 10^{-3}$  mol/L). The concentration of the receptor molecules in the buffer of Tris-HCl in  $V_{\text{DMF}}: V_{\text{Water}}$  (9/1, v/v, pH = 7.20) was diluted with a mixture of  $V_{\text{DMF}}: V_{\text{Water}} = 9:1$  to ensure a concentration of  $1 \times 10^{-5}$  mol/L. The metal ions used were metal nitrates ( $\text{Li}^+$ ,  $\text{Na}^+$ ,  $\text{K}^+$ ,  $\text{Mg}^{2+}$ ,  $\text{Ca}^{2+}$ ,  $\text{Sr}^{2+}$ ,  $\text{Ba}^{2+}$ ,  $\text{Cr}^{3+}$ ,  $\text{Fe}^{3+}$ ,  $\text{Co}^{2+}$ ,  $\text{Ni}^{2+}$ ,  $\text{Cu}^{2+}$ ,  $\text{Zn}^{2+}$ ,  $\text{Cd}^{2+}$ ,  $\text{Ag}^+$  and  $\text{Al}^{3+}$ ) and the solvent was  $V_{\text{DMF}}: V_{\text{Water}} = 9:1$  solution ( $1 \times 10^{-2}$  mol/L), the amount of metal ions added in the sample was 20 times of that of the chemical sensor **H<sub>2</sub>LS**. The titration curves were determined by the cumulative addition of  $\text{Cu}^{2+}$  and  $\text{Al}^{3+}$ , drop by drop. All experiments were conducted at room temperature. The testing conditions of all experiments were consistent: EX WL: 310.0 nm, EM WL: 388.0 nm, EX slit: 10.0 nm, EM Slit: 10.0 nm.

### 2.3.3 Method of pH measurement

The pH value was measured at room temperature by using the pH meter of model PHS-45. The pH value was adjusted in 1 mM Tris-HCl buffer solution with 1 M hydrochloric acid and 1 M tetrabutylammonium hydroxide solution.

### 2.3.4 Test experiment of **H<sub>2</sub>LS** chemical sensor on tap water sample

The fluorescence spectra of  $\text{Cu}^{2+}$  and  $\text{Al}^{3+}$  were determined by adding known amounts of  $\text{Cu}^{2+}$  and  $\text{Al}^{3+}$  to the tap water samples, tested five times in each sample, and the concentrations of  $\text{Cu}^{2+}$  and  $\text{Al}^{3+}$  were measured according to the calibration curves obtained from the fluorescence titration experiment.

### 2.3.5 Preparation of test paper

The filter paper was first soaked in 1 mol/L dilute hydrochloric acid, then dipped in distilled water for three times and washed to neutral. After vacuum drying, the filter paper was cut into a 5×1 cm filter paper piece, containing chemical sensor **H<sub>2</sub>LS** ( $V_{\text{DMF}}: V_{\text{Water}} = 9:1$ ,  $c = 1 \times 10^{-3}$  mol/L) solution is loaded on the filter paper, and then dried in vacuum. Under the UV light, the filter paper itself emits bright green fluorescence. The dried filter paper was directly applied to the identification test of  $\text{Cu}^{2+}$  in solution. It will also contain **LC** ( $V_{\text{DMF}}: V_{\text{Water}} = 9:1$ ,  $c = 1 \times 10^{-3}$  mol/L) is

loaded on the filter paper, and the dried filter paper was directly applied to the identification test of  $\text{Al}^{3+}$  in the solution.

### 3. Results and discussion

#### 3.1 Recognition of $\text{Cu}^{2+}$ by the chemical sensor

##### 3.1.1 Solvent to chemical sensor $\text{H}_2\text{Ls}$ luminescence performance study

First, the effect of the solvent system on the fluorescence intensity of the molecular sensor should be considered. The impact of different commonly used solvents on the  $\text{H}_2\text{Ls}$  fluorescence intensity of the chemical sensor were compared at an excitation wavelength of 310 nm, slit width EX = 10 nm, and EM = 10 nm (as shown in **Figure S3**).

The solvent effect is the effect of the solvent on the rate, equilibrium and even the mechanism of the reaction. In the vast majority of organic chemical reactions occurring in solvents, the nature of the solvent is extremely important not only for the reaction rate but also for the reaction equilibrium. The hallmark of a fluorescent chemical sensor is the detection of ions by changes in fluorescence intensity, so the choice of solvent for the sensor is critical. The fluorescence emission intensity of  $\text{H}_2\text{Ls}$  was measured in seven common organic solvents which could dissolve the probe  $\text{H}_2\text{Ls}$ , the results show that the fluorescence intensity of  $\text{H}_2\text{Ls}$  in DMF is relatively strong. Then select DMF as the solvent for future experiments [53-59].

##### 3.1.2 Study of water content on the luminescence performance of chemical sensor $\text{H}_2\text{Ls}$

In order to study the fluorescence intensity of the chemical sensor  $\text{H}_2\text{Ls}$  in the aqueous system, the fluorescence intensity of the chemical sensor  $\text{H}_2\text{Ls}$  in the system with different water ratios was detected (as shown in **Figure S4**). The results showed that the fluorescence intensity of the chemical sensor  $\text{H}_2\text{Ls}$  gradually decreased as the water content of the system increased. After the water content exceeded 70%, flocculation began to appear in the system, proving that excess water content has a

more significant effect on the solubility of the sensor molecules. The chemical sensor fluorescence intensity is most vigorous in the  $V_{\text{DMF}}: V_{\text{Water}} = 9:1$  system. The  $V_{\text{DMF}}: V_{\text{Water}} = 9:1$  solvent system was then selected as the solvent for later experiments [60].

### 3.1.3 Study of the recognition performance of chemical sensor **H<sub>2</sub>Ls** on $\text{Cu}^{2+}$

The fluorescence spectral characteristics of the chemical sensor **H<sub>2</sub>Ls** with metal ions were studied. The DMF/H<sub>2</sub>O (9/1, v/v, pH = 7.20) Tris-HCl buffer solution ( $1 \times 10^{-5}$  mol/L) of chemical sensor emitted a strong fluorescence at approximately 310 nm. The addition of 20-fold equivalent metal ions to the solution caused the maximum emission peak of **H<sub>2</sub>Ls** to disappear only when  $\text{Cu}^{2+}$  were added, while the maximum emission peak of **H<sub>2</sub>Ls** did not change significantly when other metal ions were added (**Figure 1**).

### 3.1.4 Quantitation of $\text{Cu}^{2+}$ fluorescence titrations and minimum detection limits

To investigate the quantification behavior of the chemical sensor **H<sub>2</sub>Ls** for  $\text{Cu}^{2+}$  recognition, a fluorescence titration experiment was performed (as shown in **Figure S5**). The cumulative addition of  $\text{Cu}^{2+}$  to the DMF/H<sub>2</sub>O solution of the chemical sensor **H<sub>2</sub>Ls** resulted in a gradual decrease of the maximum emission peak at 310 nm as the amount of  $\text{Cu}^{2+}$  increased, and the maximum emission peak of the sensor **H<sub>2</sub>Ls** completely disappeared when the amount of  $\text{Cu}^{2+}$  added was 2.0 times equivalent. The fluorescence intensity stabilized and did not change as the  $\text{Cu}^{2+}$  solution continued to be added. At the same time, it was observed that the color of the sensor solution changed from colorless to brown, which also provided a basis for visually detecting  $\text{Cu}^{2+}$ .

The experimental results showed that the chemical sensor **H<sub>2</sub>Ls** had good selective recognition ability for  $\text{Cu}^{2+}$  in aqueous system. This result may be due to the cavity of a specific size formed by the chemical sensor **H<sub>2</sub>Ls** itself. When the complex **Lc** is formed, the chemical sensor **H<sub>2</sub>Ls** selectively coordinated with  $\text{Cu}^{2+}$ , thus reducing the fluorescence intensity of the chemical sensor **H<sub>2</sub>Ls**. The limit of fluorescence detection (LOD) and limit of content (LOQ) of **H<sub>2</sub>Ls** to  $\text{Cu}^{2+}$  were

calculated from the titration spectra of the sensor **H<sub>2</sub>Ls**. Based on previous literature [61], the following equation was used to determine the LOD and LOQ.

$$\text{LOD} = K \times \delta/S; \text{LOQ} = 10 \times \delta/S; \delta = \sqrt{\frac{\sum (F_0 - \bar{F}_0)^2}{N-1}} \quad (N = 20); K = 3.$$

Where N, S, and F<sub>0</sub> are the measured values, slope, and fluorescence intensity of the blank solution of sensor **H<sub>2</sub>Ls**, respectively. The minimum detection limit (LOD) of sensor **H<sub>2</sub>Ls** to Cu<sup>2+</sup> was calculated to be 6.62 × 10<sup>-7</sup> M.

### 3.1.5 Anti-interference experimental determination of the fluorescent chemical sensor **H<sub>2</sub>Ls** toward Cu<sup>2+</sup>

The basic requirement of fluorescent chemical sensor is that it can selectively recognize ions. Therefore, the anti-interference experiment of Cu<sup>2+</sup> was carried out on the sensor **H<sub>2</sub>Ls**. First, Cu<sup>2+</sup> was added to the sensor **H<sub>2</sub>Ls**. Subsequently, other common metal ions were added, stirred and left for 10 min to measure the fluorescence intensity. The experimental results show that except for Al<sup>3+</sup>, other common metal ions have no obvious interference on the recognition of Cu<sup>2+</sup> by **H<sub>2</sub>Ls** (**Figure 2**). It is illustrated that the chemical sensor **H<sub>2</sub>Ls** has better anti-interference resistance to the recognition of Cu<sup>2+</sup>.

### 3.1.6 The pH response of the fluorescent chemical sensor **H<sub>2</sub>Ls** to Cu<sup>2+</sup>

To further investigate the applicable pH range of the fluorescence chemical sensor **H<sub>2</sub>Ls**, the change of the fluorescence intensity of the fluorescence chemical sensor **H<sub>2</sub>Ls** interacting with Cu<sup>2+</sup> was studied when the pH value was between 2.0 and 13.0. As shown in **Figure S6**, the change in fluorescence intensity of fluorescent chemosensor **H<sub>2</sub>Ls** between pH = 3 and 11 was insensitive, whereas, in the pH range between 3 and 8, the addition of Cu<sup>2+</sup> significantly reduced the fluorescence intensity of fluorescent chemosensor **H<sub>2</sub>Ls**. The results showed that the fluorescent chemical sensor **H<sub>2</sub>Ls** has a better ability to recognize Cu<sup>2+</sup> in the physiological pH range.

### 3.1.7 Time response of the fluorescent chemical sensor **H<sub>2</sub>Ls** to Cu<sup>2+</sup>

In order to investigate the response time of the fluorescent chemical sensor **H<sub>2</sub>Ls** to Cu<sup>2+</sup>, the response time of the fluorescent chemical sensor **H<sub>2</sub>Ls** to Cu<sup>2+</sup> was further studied. As shown in **Figure S7**, the experimental results showed that the response time of sensor receptor molecule **H<sub>2</sub>Ls** to Cu<sup>2+</sup> was about 10s. This result suggested that sensor **H<sub>2</sub>Ls** can quickly recognize Cu<sup>2+</sup> in aqueous systems.

### 3.1.8 Determination of the Job curve of the fluorescent chemical sensor **H<sub>2</sub>Ls** with Cu<sup>2+</sup>

To further determine the optimal ratio between the **H<sub>2</sub>Ls** and Cu<sup>2+</sup> of the fluorescence chemical sensor, the working curve of the **H<sub>2</sub>Ls** and Cu<sup>2+</sup> of the fluorescence chemical sensor was determined and plotted. As shown in **Figure S8**, the fluorescence intensity at approximately 397 nm of the sensor molecule showed an inflection point at a quantity fraction of 0.37 of the Cu<sup>2+</sup> ion's substance, indicating that the coordination between the fluorescent chemical sensor **H<sub>2</sub>Ls** and Cu<sup>2+</sup> has occurred according to a 1:2 chemometric ratio. The molecular ion peaks of m/z = 872.0987 (as shown in **Figure S9**) attributed to [(Ls + 2Cu<sup>2+</sup>)NO<sub>3</sub>]<sup>+</sup> can be seen from the ESI-MS spectrogram, further confirming that the fluorescent chemical sensor **H<sub>2</sub>Ls** is ligated to Cu<sup>2+</sup> according to a 1:2 coordination ratio.

### 3.1.9 Calculation of the ligand constants of **H<sub>2</sub>Ls** and Cu<sup>2+</sup> in a fluorescent chemical sensor

The fluorescence titration experiments of the fluorescent chemosensor **H<sub>2</sub>Ls** with Cu<sup>2+</sup>, combined with the results of the titration work curve, and the ligand constant of the fluorescent chemosensor **H<sub>2</sub>Ls** with Cu<sup>2+</sup> calculated by Benesi-Hildebrand equation (1) is 3.50×10<sup>10</sup> M<sup>-1</sup>, which indicated that the fluorescent chemosensor **H<sub>2</sub>Ls** had a powerful bonding ability to Cu<sup>2+</sup> (shown in **Figure S10**).

$$1/(F - F_0) = 1/(F_{\max} - F_0) \{ (K_a [M^{m+}]^n) + 1 \} \quad (1)$$

F is the intensity of the fluorescence intensity corresponding to the Cu<sup>2+</sup> concentration at 388 nm, F<sub>0</sub> is the intensity at 397 nm when the Cu<sup>2+</sup> concentration is zero, and F<sub>max</sub> is the maximum fluorescence intensity at 388 nm. [M<sup>m+</sup>] is the

concentration of  $\text{Cu}^{2+}$ , and  $n$  is the chemometric ratio of the chemical sensor **H<sub>2</sub>Ls** to  $\text{Cu}^{2+}$  [62]. Compared with other references [63-64], it was found that the binding constant of **H<sub>2</sub>Ls** for  $\text{Cu}^{2+}$  recognition is larger, which indicates that the copper(II) complex of **H<sub>2</sub>Ls** is more stable. In addition, the LOD of the chemical sensor **H<sub>2</sub>Ls** is smaller than that of other  $\text{Cu}^{2+}$  probe in the literature, indicating that the chemical sensor is more sensitive to recognize  $\text{Cu}^{2+}$ . Binding constants and detection lines between the related chemosensors mentioned in literatures were compared, as shown in **Table 1**.

**Table 1** Comparison of binding constants and detection lines between the chemosensors.

### *3.1.10 Exploration of the mechanism of $\text{Cu}^{2+}$ recognition by the fluorescent chemical sensor **H<sub>2</sub>Ls***

Based on the above experimental results, a mechanism for the  $\text{Cu}^{2+}$  ions recognition by the fluorescent chemical sensor **H<sub>2</sub>Ls** was proposed, as shown in **Figure 3**. The fluorescent chemical sensor **H<sub>2</sub>Ls** itself gives green fluorescence. The outer electron configuration of  $\text{Cu}^{2+}$  is  $d^9$ , which is paramagnetic and the formation of the complex **L<sub>C</sub>** leads to fluorescence quenching of chemical sensor **H<sub>2</sub>Ls**. According to Jahn-Teller effect, there are three electrons in the two degenerate  $d$  orbitals ( $E_g$ ) of divalent copper(II) ions in octahedral complexes due to the splitting of crystal field. The number of electrons occupied in these two orbitals is different, and the complex is a nonlinear molecule, which leads to the splitting of  $E_g$  [65]. The results of splitting lead to Jahn-Teller distortion, and the Irving-Williams (CFSE increase) order obtained from the crystal field splitting energy is abnormal, which leads to the copper(II) complexes being more stable than other bivalent metal(II) complexes in the same period. After  $\text{Cu}^{2+}$  combines with **H<sub>2</sub>Ls**, the copper(II) complex is more stable and has lower energy than **H<sub>2</sub>Ls**.

The effect of the complexes in different oxidation states on the charge density is linear, indicating that there is a strong relationship between the charge density around

the metal and the oxidation state [66-67]. In the presence of  $\text{Cu}^{2+}$ , the fluorescence intensity of the system is quenched. This indicates that  $\text{Cu}^{2+}$  interacts with the system effectively, which reduces the fluorescence intensity.

### 3.1.11 Experiments on tap water samples with $\text{Cu}^{2+}$

It was detecting  $\text{Cu}^{2+}$  in tap water with **H<sub>2</sub>LS** to explore the utility of chemical sensor **H<sub>2</sub>LS**. A test sample was first made by adding a known exact amount of  $\text{Cu}^{2+}$  to tap water. Quantitative analysis of the test samples using the standard addition method using fluorescence spectroscopy was repeated. It can be seen from **Table S1** that the average recoveries ranged from 97.6% to 104.2% with relative standard deviations within 3%. The chemical sensor **H<sub>2</sub>LS** was shown to be suitable for the quantitative detection of  $\text{Cu}^{2+}$  in tap water.

### 3.1.12 Application of test paper

Based on the fluorescence selectivity of the chemical sensor to  $\text{Cu}^{2+}$ , fluorescence detection test papers loaded with the sensor **H<sub>2</sub>LS** were fabricated. The dilute hydrochloric acid-treated filter paper was immersed in a DMF/ $\text{H}_2\text{O}$  solution of sensor **H<sub>2</sub>LS** at a concentration of  $1.0 \times 10^{-4}$  mol/L for loading. After the load was uniform, the test paper was placed in a vacuum drying chamber and dried at low temperature, and then dried paper was used for  $\text{Cu}^{2+}$  determination. Before the test, the test paper was green under UV light. After dropping the  $\text{Cu}^{2+}$  solution on the strip, the color of the test paper became colorless under the UV light, as shown in **Figure 4**.

## 3.2 Study of the recognition performance of the chemical sensor **Lc** on $\text{Al}^{3+}$

### 3.2.1 Fluorescence recognition study of metal ions by **Lc**

Through the study and exploration of the preliminary experiments, it was found that **H<sub>2</sub>LS** had a good recognition effect on  $\text{Cu}^{2+}$  in aqueous system. However, in anti-interference experiments, the presence of  $\text{Al}^{3+}$  in the system affected the recognition of  $\text{Cu}^{2+}$ . Therefore, it was envisaged that after the  $\text{Cu}^{2+}$  was recognized, the sensor will continuously recognize  $\text{Al}^{3+}$ . With this scenario in mind, the

fluorescence recognition properties of the complex **Lc** as a sensor **Lc** on various metal ions were investigated.

As shown in **Figure S11**, in the solution of the sensor **Lc** the fluorescence intensity of the sensor **Lc** changed almost nothing with the addition of other metal ions, only the fluorescence was enhanced with the addition of  $\text{Al}^{3+}$ . The sensor **Lc** has single recognition for  $\text{Al}^{3+}$ .

### 3.2.2 Anti-interference experimental study of **Lc** on $\text{Al}^{3+}$ recognition

As can be seen from the competition experiment (**Figure S12**), the recognition of **Lc** to  $\text{Al}^{3+}$  was not affected when other metal ions were present. Only the  $\text{Al}^{3+}$  can replace the  $\text{Cu}^{2+}$  in the complex **Lc** to form a new complex **Lc**. Thus, the sensor **Lc** had high selectivity and single recognition as a chemical sensor for identifying  $\text{Al}^{3+}$ .

### 3.2.3 Fluorescence titration of **Lc** against $\text{Al}^{3+}$

Fluorescence titration experiments were performed, and the minimum detection limit of **Lc** for  $\text{Al}^{3+}$  was calculated, as shown in **Figure S13**. The intensity of the emission peak of **Lc** increased with the constant addition of  $\text{Al}^{3+}$  until the emission spectrum does not change with the addition of 3.0 equivalents of  $\text{Al}^{3+}$ . The results showed that the  $\text{Cu}^{2+}$  in the complex **Lc** were utterly replaced by  $\text{Al}^{3+}$  and formed **Lc**- $\text{Al}^{3+}$ . Thus, the fluorescence intensity gradually increased.

At the same time, the binding equilibrium constant ( $K_2 = 3.05 \times 10^{11} \text{ M}^{-1}$ ) of **Lc** to  $\text{Al}^{3+}$  was calculated based on linear fitting (**Figure S18**), and it was found that the binding equilibrium constant of **H<sub>2</sub>Ls** to  $\text{Al}^{3+}$  was ten times higher than that of **H<sub>2</sub>Ls** to  $\text{Cu}^{2+}$ . Besides, the minimum detection limit of **Lc** for  $\text{Al}^{3+}$  is  $5.33 \times 10^{-7} \text{ M}$ . Reference to other literature [68-69], comparison of binding constants and detection lines between the chemosensors as shown in **Table 1**.

### 3.2.4 The pH response of the fluorescent chemical sensor **Lc** to $\text{Al}^{3+}$

To further investigate the applicable pH range of the fluorescence chemical sensor **Lc**, the change of the fluorescence intensity of the fluorescence chemical

sensor **Lc** interacting with  $\text{Al}^{3+}$  was studied when the pH value was between 2 and 13. As shown in **Figure S14**, the change in fluorescence intensity of fluorescent chemosensor **Lc** between pH = 4 and 11 was insensitive, whereas, in the pH range between 5 and 8, the addition of  $\text{Al}^{3+}$  significantly enhanced the fluorescence intensity of fluorescent chemosensor **Lc**. The results show that the fluorescent chemical sensor **Lc** has a better ability to recognize  $\text{Al}^{3+}$  in the neutral pH range.

### 3.2.5 Time response of the fluorescent chemical sensor **Lc** to $\text{Al}^{3+}$

In order to investigate the response time of the fluorescent chemical sensor **Lc** to  $\text{Al}^{3+}$ , the response time of the fluorescent chemical sensor **Lc** to  $\text{Al}^{3+}$  was further studied. As shown in **Figure S15**, the experimental results show that the response time of sensor receptor molecule **Lc** to  $\text{Al}^{3+}$  is about 20 s. This result suggests that sensor **Lc** can quickly recognize  $\text{Al}^{3+}$  in systems.

### 3.2.6 Determination of Job curves of **Lc** versus $\text{Al}^{3+}$

Working curves of **Lc** and  $\text{Al}^{3+}$  were plotted to determine further the optimal ratio of **Lc** and  $\text{Al}^{3+}$ . As shown in **Figure S16**, the fluorescence intensity of the sensor molecule appeared a turning point at the mass fraction of 0.75 for  $\text{Al}^{3+}$ . This result indicated that the fluorescence chemical sensor **Lc** was coordinated with the  $\text{Al}^{3+}$ , according to the stoichiometry of 1:3. The molecular ion peaks of  $m/z = 819.2246$  (as shown in **Figure S17**) attributed to  $[(\text{L}_s+3\text{Al}^{3+})\cdot\text{H}_2\text{O}\cdot\text{DMF}]^{7+}$  can be seen from the ESI-MS spectrogram, further verifying that the **Lc** and  $\text{Al}^{3+}$  were ligated according to a 1:3 coordination ratio.

### 3.2.7 Exploration of the mechanism of $\text{Al}^{3+}$ ion recognition by **Lc**

The mechanism of **Lc** recognition of  $\text{Al}^{3+}$  is proposed based on the above experimental results, as shown in **Figure 5**. The outer electron configuration of  $\text{Al}^{3+}$  is  $p^6$ , and the p orbital is full, which forms a one-dimensional plane  $[(\text{L}_s+3\text{Al}^{3+})\cdot\text{H}_2\text{O}\cdot\text{DMF}]^{7+}$  due to the addition of  $\text{Al}^{3+}$ , and the chelation-enhanced fluorescence (CHEF) is the main reason for the enhanced fluorescence [70-71]. In the

presence of  $\text{Al}^{3+}$ , the fluorescence intensity of the system is enhanced, which means that the copper(II) complex of **H<sub>2</sub>Ls** as a quenched fluorescent group is activated at the presence of  $\text{Al}^{3+}$  in water system, which improves the fluorescence intensity of **Lc**. In addition, the planarity of the complex structure is also enhanced, leading to a strong PET (photoinduced electron transfer) from the receptor, which further enhances the fluorescence emission [72-73].

### 3.2.8 Application of test paper

Based on the fluorescence selectivity of the chemical sensor **Lc** to  $\text{Al}^{3+}$ , fluorescence detection test papers loaded with the sensor **Lc** were fabricated. The dilute hydrochloric acid-treated filter paper was immersed in a DMF/ $\text{H}_2\text{O}$  solution of the copper(II) complex of **H<sub>2</sub>Ls** at a concentration of  $1.0 \times 10^{-4}$  mol/L for loading. After the load was uniform, the test paper was placed in a vacuum drying chamber and dried at low temperature, and then dried paper was used for  $\text{Al}^{3+}$  determination. Before the test, the test paper was colorless under UV light. After dropping the  $\text{Al}^{3+}$  solution on the strip, the color of the test paper became green under the UV light, as shown in **Figure 4**.

## 4. Conclusion

In this paper,  $\text{Cu}^{2+}$  was first detected by using a bis(salamo)-like tetraoxime chemical sensor **H<sub>2</sub>Ls**. The experimental results showed that the sensor **H<sub>2</sub>Ls** can detect  $\text{Cu}^{2+}$  in aqueous solution by the fluorescence quenching phenomenon. The advantages of the sensor **H<sub>2</sub>Ls** for detection of  $\text{Cu}^{2+}$  are a low detection limit, high coordination constant, a wide pH range (3.0~8.0), and fast response time (about 10 seconds). A test paper loaded with the sensor **H<sub>2</sub>Ls** has been prepared for the detection of  $\text{Cu}^{2+}$  in aqueous solution easily, quickly, accurately and qualitatively. Therefore, this fluorescent chemical sensor has potential applications for detecting  $\text{Cu}^{2+}$  in real life. Besides, the sensor **Lc** can identify  $\text{Al}^{3+}$  in the system and achieves interference-free identification of  $\text{Al}^{3+}$  by other trivalent metals.

### Conflicts of Interest

The authors declare no competing financial interests.

### Acknowledgments

This work was supported by the National Natural Science Foundation of China (21761018), Science and Technology Program of Gansu Province (18YF1GA054), and the Program for Excellent Team of Scientific Research in Lanzhou Jiaotong University (201706), three of which are gratefully acknowledged.

### References

- [1] S. Zeng, S.J. Li, T.T. Liu, X.J. Sun, Z.Y. Xing, A significant fluorescent "turn-on" chemosensor for  $\text{Al}^{3+}$  detection and application in real sample, logic gate and bioimaging, *Inorg. Chim. Acta.* 495 (2019) 1873-3255.
- [2] Y. Xu, L. Yang, H. Wang, Y. Zhang, X. Yang, M. Pei, G. Zhang, A new "off-on-off" sensor for sequential detection of  $\text{Al}^{3+}$  and  $\text{Cu}^{2+}$  with excellent sensitivity and selectivity based on different sensing mechanisms, *J. Photochem. Photobiol. A* 391 (2020) 1010-6030.
- [3] Y. Wu, X. Wen, Z. Fan, Selective and Sensitive Fluorescence Probe for Detection of  $\text{Al}^{3+}$  in Food Samples Based on Aggregation-Induced Emission and Its Application for Live Cell Imaging, *Food. Anal. Methods* 12 (2019) 1736-1746.
- [4] J.H. Wang, Y.M. Liu, J.B. Chao, H. Wang, Y. Wang, S. Shuang, A simple but efficient fluorescent sensor for ratiometric sensing of  $\text{Cd}^{2+}$  and bio-imaging studies, *Sens. Actuators B* 303 (2020) 127216.
- [5] C. Varadaraju, M.S. Paulraj, G. Tamilselvan, I.V.M.V. Enoch, V. Srinivasadesikan, L. Shyi-Long, Evaluation of metal ion sensing behaviour of fluorescent probe along with its precursors: PET-CHEF mechanism, molecular logic gate behaviour and DFT studies, *J. Incl. Phenom. Macrocycl. Chem.* 95 (2019) 79-89.
- [6] P.G. Sutariya, H. Soni, S.A. Gandhi, A. Pandya, Luminescent behavior of pyrene-allied calix 4 arene for the highly pH-selective recognition and determination of  $\text{Zn}^{2+}$ ,  $\text{Hg}^{2+}$  and  $\text{I}^-$  via the CHEF-PET mechanism: computational experiment and paper-based device, *New J. Chem* 43 (2019) 9855-9864.

- [7] P.G. Sutariya, H. Soni, S.A. Gandhi, A. Pandya, Novel tritopic calix 4 arene CHEF-PET fluorescence paper based probe for  $\text{La}^{3+}$ ,  $\text{Cu}^{2+}$ , and  $\text{Br}^-$ : Its computational investigation and application to real samples, *J. Lumin.* 212 (2019) 171-179.
- [8] S. Slassi, M. Aarjane, A. El-Ghayoury, A. Amine, A highly turn-on fluorescent CHEF-type chemosensor for selective detection of  $\text{Cu}^{2+}$  in aqueous media, *Spectrochim. Acta A* 215 (2019) 348-353.
- [9] S. Saha, S. Das, P. Sahoo, Highly Selective Optical and Fluorescence "Turn On" Signaling of  $\text{Al}^{3+}$ : Cell Imaging and Estimation in Rice Plant, *Chemistryselect* 4 (2019) 13968-13973.
- [10] V. Raju, R.S. Kumar, Y. Tharakeswar, S.K.A. Kumar, A multifunctional Schiff-base as chromogenic chemosensor for  $\text{Mn}^{2+}$  and fluorescent chemosensor for  $\text{Zn}^{2+}$  in semi-aqueous environment, *Inorg. Chim. Acta.* 493 (2019) 49-56.
- [11] S. Mondal, S.M. Mandal, D. Ojha, D. Chattopadhyay, C. Sinha, Water soluble sulfaguanidine based Schiff base as a "Turn-on" fluorescent probe for intracellular recognition of  $\text{Zn}^{2+}$  in living cells and exploration for biological activities, *Polyhedron* 172 (2019) 28-38.
- [12] A. Asaithambi, D. Okada, G. Prinz, H. Sato, A. Saeki, T. Nakamura, T. Nabeshima, Y. Yamamoto, A. Lorke, Polychromatic Photoluminescence of Polymorph Boron Dipyrromethene Crystals and Heterostructures, *J. Phys. Chem.* 123 (2018) 5061-5066.
- [13] T. Hojo, R. Matsuoka, T. Nabeshima, A Conformationally Flexible Macrocyclic Dipyrin Tetramer and Its Unsymmetrically Twisted Luminescent Zinc(II) Complex, *Inorg. Chem.* 58 (2019) 995-998.
- [14] T. Hojo, T. Nakamura, R. Matsuoka, T. Nabeshima, Uniquely folded shapes, photophysical properties, and recognition abilities of macrocyclic BODIPY oligomers, *Heteroatom Chem.* 29 (2018) e21470.
- [15] A. Nagai, T. Nakamura, T. Nabeshima, A twisted macrocyclic hexanuclear palladium complex with internal bulky coordinating ligands, *Chem. Commun.* 55 (2019) 2421-2424.
- [16] T. Nakamura, Y. Kawashima, E. Nishibori, T. Nabeshima, Bpytrisalen/Bpytrisaloph: A Triangular Platform That Spatially Arranges Different Multiple Labile Coordination Sites, *Inorg. Chem.* 58 (2019) 7863-7872.
- [17] S. Maity, M. Shyamal, R. Maity, N. Mudi, P. Hazra, P.K. Giri, S.S. Samanta, S. Pyne, A. Misra, An antipyrene based fluorescent probe for distinct detection of  $\text{Al}^{3+}$  and  $\text{Zn}^{2+}$  and its

- AIEE behaviour, *Photochem. Photobiol. Sci.* 19 (2020) 681-694.
- [18] T. Nakamura, S. Tsukuda, T. Nabeshima, Double-Circularly Connected Saloph-Belt Macrocycles Generated from a Bis-Armed Bifunctional Monomer, *J. Am. Chem. Soc.* 141 (2019) 6462-6467.
- [19] M. Saikawa, T. Noda, R. Matsuoka, T. Nakamura, T. Nabeshima, Heterodinuclear Group 13 Element Complexes of N<sub>4</sub>O<sub>6</sub>-Type Dipyrin with an Unsymmetrical Twisted Structure, *Eur. J. Inorg. Chem.* 6 (2019) 766-769.
- [20] L. Wang, Z.L. Wei, C. Liu, W.K. Dong, J.X. Ru, Synthesis and characterization for a highly selective bis(salamo)-based chemical sensor and imaging in living cell, *Spectrochim. Acta A* 239 (2020) 118496.
- [21] C. Liu, Z.L. Wei, H.R. Mu, W.K. Dong, Y.J. Ding, A novel unsymmetric bis(salamo)-based chemosensor for detecting Cu<sup>2+</sup> and continuous recognition of amino acids, *J. Photochem. Photobio. A* 397 (2020) 112569.
- [22] X.Y. Dong, Q.P. Kang, X.Y. Li, J.C. Ma, W.K. Dong, Structurally characterized solvent-induced homotrimeric cobalt(II) N<sub>2</sub>O<sub>2</sub>-donor bisoxime-type complexes, *Crystals* 8 (2018) 139.
- [23] Y.D. Peng, X.Y. Li, Q.P. Kang, Y. Zhang, W. K. Dong, Synthesis and fluorescence properties of asymmetrical salamo-type tetranuclear zinc(II) complex, *Crystals* 8 (2018) 107.
- [24] X.X. An, Z.Z. Chen, H.R. Mu, L. Zhao, Investigating into crystal structures and supramolecular architectures of four newly synthesized hetero-octanuclear [Cu<sup>II</sup><sub>4</sub>-Ln<sup>III</sup><sub>4</sub>] (Ln = Sm, Eu, Tb and Dy) complexes produced by a hexadentate bisoxime chelate ligand, *Inorg. Chim. Acta* 511 (2020) 119823.
- [25] X.Y. Li, Q.P. Kang, C. Liu, Y. Zhang, W.K. Dong, Structurally characterized homo-trinuclear Zn<sup>II</sup> and hetero-pentanuclear [Zn<sup>II</sup><sub>4</sub>Ln<sup>III</sup>] complexes constructed from an octadentate bis(Salamo)-based ligand: Hirshfeld surfaces, fluorescence and catalytic properties, *New J. Chem.* 43 (2019) 4605-4619.
- [26] X.X. An, Q. Zhao, H.R. Mu, W.K. Dong, A new half-salamo-based homo-trinuclear nickel(II) complex: Crystal structure, Hirshfeld surface analysis, and fluorescence properties, *Crystals* 9 (2019) 101.
- [27] C. Liu, X.X. An, Y.F. Cui, K.F. Xie, W.K. Dong, Novel structurally characterized hetero-

- bimetallic [Zn(II)<sub>2</sub>M(II)] (M = Ca and Sr) bis(salamo)-type complexes: DFT calculation, Hirshfeld analyses, antimicrobial and fluorescent properties, *Appl. Organomet. Chem.* 34 (2020) e5272.
- [28] S. Yonemura, T. Nakamura, T. Nabeshima, Threading/Folding Recognition Modes of Phosphodiester by a p-Nitrophenylamide Cyclodextrin Derivative, *Chem. Lett.* 49 (2020) 493-496.
- [29] L.W. Zhang, Y. Zhang, Y.F. Cui, M. Yu, W.K. Dong, Heterobimetallic [Ni<sup>II</sup>Ln<sup>III</sup>] (Ln = Sm and Tb) N<sub>2</sub>O<sub>4</sub>-donor coordination polymers: syntheses, crystal structures and fluorescence properties, *Inorg. Chim. Acta* 506 (2020) 119534.
- [30] H.R. Mu, X.X. An, C. Liu, Y. Zhang, W.K. Dong, Structurally characterized self-assembled heterobimetallic Ni(II)-Eu(III)-salamo-bipyridine coordination polymer: Synthesis, photophysical and antimicrobial properties, *J. Struct. Chem.* 61 (2020) 1218-1229.
- [31] Y. Zhang, M. Yu, Y.Q. Pan, Y. Zhang, L. Xu, X.Y. Dong, Three rare heteromultinuclear 3d-4f salamo-like complexes constructed from auxiliary ligand 4,4'-bipy: Syntheses, structural characterizations, fluorescence and antimicrobial properties, *Appl. Organomet. Chem.* 34 (2020) e5442.
- [32] L. Wang, Y.Q. Pan, J.F. Wang, Y. Zhang, Y.J. Ding, A highly selective and sensitive half-salamo-based fluorescent chemosensor for sequential detection of Pb(II) ion and Cys, *J. Photochem. Photobiol. A*, 400 (2020) 112719.
- [33] Y.Q. Pan, Y. Zhang, M. Yu, Y. Zhang, L. Wang, Newly synthesized homomultinuclear Co (II) and Cu (II) bis-salamo-like complexes: structural characterizations, Hirshfeld analyses, fluorescence and antibacterial properties, *Appl. Organomet. Chem.* 34 (2020) e5441.
- [34] M. Yu, Y. Zhang, Y.Q. Pan, L. Wang, Two novel copper (II) salamo-based complexes: syntheses, X-ray crystal structures, spectroscopic properties and Hirshfeld surfaces analyses, *Inorg. Chim. Acta* 509 (2020) 119701.
- [35] F. Wang, L. Gao, Q. Zhao, Y. Zhang, W.K. Dong, Y.J. Ding, A highly selective fluorescent chemosensor for CN<sup>-</sup> based on a novel bis(salamo)-type tetraoxime ligand, *Spectrochim. Acta A* 190 (2018) 111-115.
- [36] Y.Q. Pan, X. Xu, Y. Zhang, Y. Zhang, W.K. Dong, A highly sensitive and selective bis(salamo)-type fluorescent chemosensor for identification of Cu<sup>2+</sup> and the continuous

- recognition of  $S^{2-}$ , arginine and lysine, *Spectrochim. Acta A* 229 (2020) 117927.
- [37] Z.L. Wei, L. Wang, J.F. Wang, W.T. Guo, Y. Zhang, W. K. Dong, Two highly sensitive and efficient salamo-like copper(II) complex sensors for recognition of  $CN^-$ , *Spectrochim. Acta A* 228 (2020) 117775.
- [38] V. Kumar, S. Kundu, B. Sk, A. Patra, A naked-eye colorimetric sensor for methanol and 'turn-on' fluorescence detection of  $Al^{3+}$ , *New J. Chem.* 43 (2019) 18582-18589.
- [39] L.M. Pu, X.Y. Li, J. Hao, Y.X. Sun, Y. Zhang, H.T. Long, W.K. Dong, Exploration and application of a highly sensitive bis(salamo)-based fluorescent sensor for  $B_4O_7^{2-}$  in water-containing systems and living cells, *Sci. Rep.* 8 (2018) 14058.
- [40] W.K. Dong, S.F. Akogun, Y. Zhang, Y.X. Sun, X.Y. Dong, A reversible "turn-on" fluorescent sensor for selective detection of  $Zn^{2+}$ , *Sens. Actuators B* 238 (2017) 723-734.
- [41] W.K. Dong, X.L. Li, L. Wang, Y. Zhang, Y.J. Ding, A new application of salamo-type bisoximes: as a relay-sensor for  $Zn^{2+}/Cu^{2+}$  and its novel complexes for successive sensing of  $H^+/OH^-$ , *Sens. Actuators B* 229 (2016) 370-378.
- [42] L. Wang, Z.L. Wei, Z.Z. Chen, C. Liu, W. K. Dong, Y. J. Ding, A chemical sensor capable for fluorescent and colorimetric detection to  $Cu^{2+}$  and  $CN^-$  based on coordination and nucleophilic addition mechanism, *Microchem. J.* 155 (2020) 104801.
- [43] Q.P. Kang, X.Y. Li, L. Wang, Y. Zhang, W.K. Dong, Containing-PMBP  $N_2O_2$ -donors transition metal (II) complexes: synthesis, crystal structure, Hirshfeld surface analyses and fluorescence properties, *Appl. Organomet. Chem.* 33 (2019) e5013.
- [44] J. Hao, X.Y. Li, Y. Zhang, W.K. Dong, A reversible bis(salamo)-based fluorescence sensor for selective detection of  $Cd^{2+}$  in water-containing systems and food samples, *Materials* 11 (2018) 523.
- [45] Q.P. Kang, X.Y. Li, Z.L. Wei, Y. Zhang, W.K. Dong, Symmetric containing-PMBP  $N_2O_2$ -donors nickel(II) complexes: syntheses, structures, Hirshfeld analyses and fluorescent properties, *Polyhedron* 165 (2019) 38-50.
- [46] Q. Zhao, X.X. An, L.Z. Liu, W.K. Dong, Syntheses, luminescences and Hirshfeld surfaces analyses of structurally characterized homo-trinuclear  $Zn^{II}$  and hetero-pentanuclear  $Zn^{II}$ - $Ln^{III}$  ( $Ln=Eu, Nd$ ) bis(salamo)-like complexes, *Inorg. Chim. Acta* 490 (2019) 6-15.

- [47] L.Z. Liu, M. Yu, X.Y. Li, Q.P. Kang, W.K. Dong, Syntheses, structures, Hirshfeld analyses and fluorescent properties of two Ni(II) and Zn(II) complexes constructed from a bis(salamo)-like ligand, *Chin. J. Inorg. Chem.* 35 (2019) 1283-1294.
- [48] J.C. Ma, X.Y. Dong, W.K. Dong, Y. Zhang, L.C. Zhu, J.T. Zhang, An unexpected dinuclear Cu(II) complex with a bis(Salamo) chelating ligand: Synthesis, crystal structure, and photophysical properties, *J. Coord. Chem.* 69 (2016) 149-159.
- [49] H.R. Mu, M. Yu, L. Wang, Y. Zhang Y.J. Ding, Catching  $S^{2-}$  and  $Cu^{2+}$  by a highly sensitive and efficient salamo-like fluorescence-ultraviolet dual channel chemosensor, *Phosphorus Sulfur Silicon Relat. Elem.* 195 (2020) 730-739.
- [50] Y.X. Sun, Y.Q. Pan, X. Xu, Y. Zhang, Unprecedented dinuclear  $Cu^{II}$  N,O-donor complex: Synthesis, structural characterization, fluorescence property, and Hirshfeld analysis. *Crystals* 9 (2019) 607.
- [51] L.Z. Liu, L. Wang, M. Yu, Q. Zhao, Y. Zhang, Y.X. Sun, W. K. Dong, A highly sensitive and selective fluorescent "off-on-off" relay chemosensor based on a new bis(salamo)-type tetraoxime for detecting  $Zn^{2+}$  and  $CN^-$ , *Spectrochim. Acta A* 222 (2019) 117209.
- [52] Y. Zhang, L.Z. Liu, Y.D. Peng, N. Li, W.K. Dong, Structurally characterized trinuclear nickel(II) and copper(II) salamo-type complexes: syntheses, Hirshfeld analyses and fluorescent properties, *Transit. Met. Chem.* 44 (2019) 627-639.
- [53] S. Khanra, S. Ta, M. Ghosh, S. Chatterjee, D. Das, Subtle structural variation in azine/imine derivatives controls  $Zn^{2+}$  sensitivity: ESIPT-CHEF combination for nano-molar detection of  $Zn^{2+}$  with DFT support, *Rsc Advances* 9 (2019) 21302-21310.
- [54] S.Z. Zhang, J. Chang, H.J. Zhang, Y.X. Sun, Y. Wu, Y.B. Wang, Synthesis, crystal structure and spectral properties of binuclear Ni(II) an Cubane-like  $Cu_4(\mu_3-O)_4$  cored tetranuclear Cu(II) complexes based on coumarin Schiff base, *Chin. J. Inorg. Chem.* 36 (2020) 503-514.
- [55] J. Chang, S.Z. Zhang, Y. Wu, H.J. Zhang, Y.X. Sun, Three supramolecular trinuclear nickel(II) complexes based on Salamo-type chelating ligand: syntheses, crystal structures, solvent effect, Hirshfeld surface analysis and DFT calculation, *Transit. Met. Chem.* 45 (2020) 279-293.
- [56] B. Das, A. Jana, A. Das Mahapatra, D. Chattopadhyay, A. Dhara, S. Mabhai, S. Dey, Fluorescein derived Schiff base as fluorimetric zinc (II) sensor via 'turn on' response and its

- application in live cell imaging, *Spectrochim. Acta A* 212 (2019) 222-231.
- [57] J.B. Chae, H. Lee, C. Kim, Determination of Zinc Ion by a Quinoline-Based Fluorescence Chemosensor, *Journal of Fluorescence* 30 (2020) 347-356.
- [58] K. Aich, S. Das, S. Gharami, L. Patra, T.K. Mondal, Two New Quinoline-Benzothiazole Blended 'Off-On' Type Fluorescent Probes Exclusively Detect  $\text{Cd}^{2+}$ , *Chemistryselect* 4 (2019) 8068-8073.
- [59] T.W. Chen, U. Rajaji, S.M. Chen, J.Y. Wang, Z.A. Allothman, M.A. Ali, S.M. Wabaidur, F.A. Hemaïd, S.Y. Lee, W.H. Chang, Sonochemical preparation of carbon nanosheets supporting cuprous oxide architecture for high-performance and non-enzymatic electrochemical sensor in biological samples, *Ultrason. Sonochem.* 66 (2020) 1350-4177.
- [60] G.J. Park, H. Kim, J.J. Lee, Y.S. Kim, S.Y. Lee, S. Lee, I. Noh, C. Kim, A highly selective turn-on chemosensor capable of monitoring  $\text{Zn}^{2+}$  concentrations in living cells and aqueous solution, *Sens. Actuators B* 215 (2015) 568-576.
- [61] S. Nandi, A. Sahana, B. Sarkar, S.K. Mukhopadhyay, D. Das, Pyridine Based Fluorescence Probe: Simultaneous Detection and Removal of Arsenate from Real Samples with Living Cell Imaging Properties, *Journal of Fluorescence* 25 (2015) 1191-1201.
- [62] S. Mukherjee, S. Talukder, A Reversible Pyrene-based Turn-on Luminescent Chemosensor for Selective Detection of  $\text{Fe}^{3+}$  in Aqueous Environment with Logic Gate Application, *Journal of Fluorescence* 26 (2016) 1021-1028.
- [63] M. Tian, H. He, B.B. Wang, X. Wang, Y. Liu, F.L. Jiang, A reaction-based turn on fluorescence sensor for the detection of Cu(II) with excellent sensitivity and selectivity: Synthesis, DFT calculations, kinetics and application in real water samples, *Dyes Pigm.* 165 (2019) 383-390.
- [64] M. Sahu, A. Kumar Manna, K. Rout, J. Modal, G.K. Patra, A highly selective thiosemicarbazonebased Schiff base chemosensor for colorimetric detection of  $\text{Cu}^{2+}$  and  $\text{Ag}^+$  ions and turn-on fluorometric detection of  $\text{Ag}^+$  ions, *Inorg. Chim. Acta* 508 (2020) 119633.
- [65] L. Li, Y. Shen, Y.H. Zhao, L. Mu, X. Zeng, C. Redshaw, G. Wei, A single chemosensor for multiple analytes: Fluorogenic and ratiometric absorbance detection of  $\text{Zn}^{2+}$ ,  $\text{Mg}^{2+}$  and  $\text{F}^-$ , and its cell imaging, *Sens. Actuators B* 226 (2016) 279-288.
- [66] H.J. Daniela Soledad, H.H. Jose Guadalupe, H.A. Carlos Alberto, T. Pandiyan, Novel insight

- of indium(III) complex of N, N'-bis(salicylidene)ethylenediamine as chemo-sensor for selective recognition of  $\text{HSO}_4^-$  and hemolytic toxicity (Red Blood Cells) studies: Experimental and theoretical studies, *Sens. Actuators B* 293 (2019) 357-365.
- [67] H.A. Carlos Alberto, R.G. Brayan, T. Pandiyan, N. Jayanthi, S. Narinder, Simultaneous recognition of cysteine and cytosine using thiophene-based organic nanoparticles decorated with Au NPs and bio-imaging of cells, *Photochem. Photobiol. Sci.* 18 (2019) 1761.
- [68] K.S. Shen, S.S. Mao, X.K. Shi, F. Wang, Y.L. Xu, S.O. Aderinto, H.L. Wu, Characterization of a highly  $\text{Al}^{3+}$ -selective fluorescence probe based on naphthalimide-Schiff base and its application to practical water samples, *Luminescence* 1 (2017) 54-63.
- [69] H.P. Peng, K.S. Shen, S.S. Mao, X.K. Shi, Y.L. Xu, S.O. Aderinto, H.L. Wu, A highly selective and sensitive fluorescent turn-on probe for  $\text{Al}^{3+}$  based on naphthalimide Schiff base, *J. Fluores.* 27 (2017) 1191-1200.
- [70] H.A. Carlos Alberto, T. Pandiyan, R. Pushap, S. Narinder, Z. Rodolfo, Fluorescent organic nanoparticles (FONs) for the selective recognition of  $\text{Zn}^{2+}$ : Applications to multi-vitamin formulations in aqueous medium, *Sens. Actuators B* 223 (2016) 59-67.
- [71] H.A. Carlos Alberto, R. Pushap, T. Pandiyan, S. Narinder, Fluorescent organic nanoparticles (FONs) for selective recognition of  $\text{Al}^{3+}$ : application to bio-imaging for bacterial sample, *RSC Advances* 44 (2016) 37944-37952.
- [72] J.A.O. Granados, P. Thangarasu, N. Singh, J. M. Vazquez-Ramos, Tetracycline and its quantum dots for recognition of  $\text{Al}^{3+}$  and application in milk developing cells bio-imaging, *Food Chem.* 278 (2019) 523-532.
- [73] C. A. Huerta-Aguilar, T. Pandiyan, N. Singh, N. Jayanthi, Three novel input logic gates supported by fluorescence studies: organic nanoparticles (ONPs) as chemo-sensor for detection of  $\text{Zn}^{2+}$  and  $\text{Al}^{3+}$  in aqueous medium, *Spectrochim. Acta A* 146 (2015) 142-150.

## Author Biographies

**Ruo-Nan Bian** is currently pursuing her master's degree in the School of Chemical and Biological Engineering at Lanzhou Jiaotong University, China. She obtained her B.S. in the School of Chemical and Biological Engineering at Lanzhou Jiaotong University, China, in 2017.

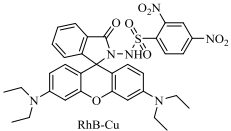
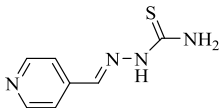
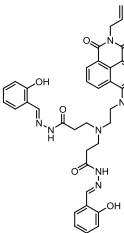
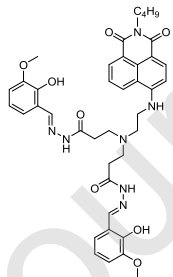
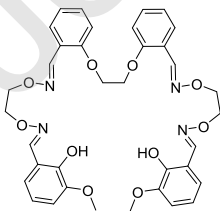
**Ji-Fa Wang** is currently pursuing his master's degree in the School of Chemical and Biological Engineering at Lanzhou Jiaotong University, China. He obtained his B.S. in the School of Materials Science and Engineering at Qilu University of Technology, China, in 2018.

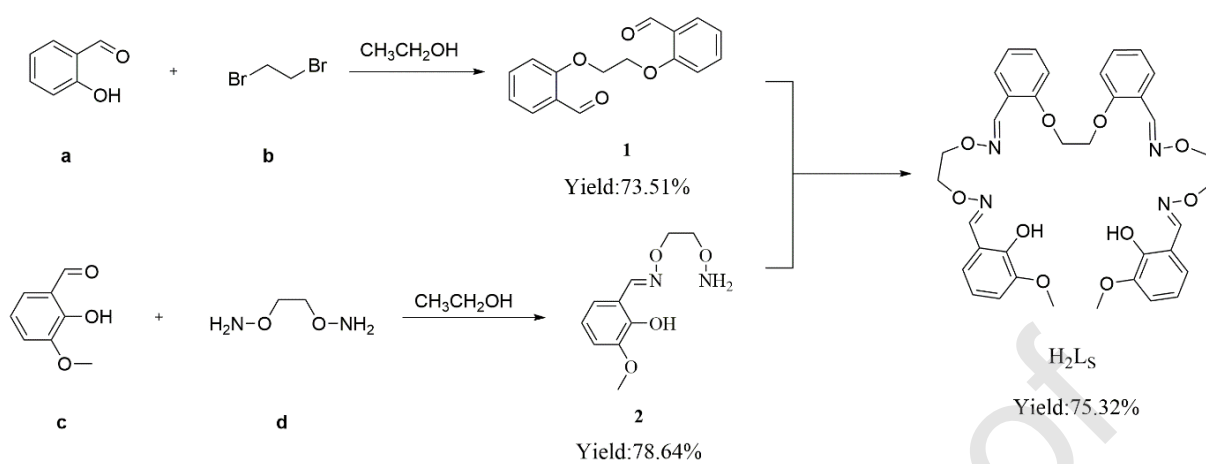
**Ya-Juan Li** is currently pursuing her master's degree in the School of Chemical and Biological Engineering at Lanzhou University, China. She obtained her B.S. in the School of chemical engineering and technology, at Tianshui Normal University, China, in 2018.

**Yang Zhang** received his PhD degree in 2019 from Lanzhou Jiaotong University, China. He is a lecturer in the school of chemistry and bioengineering of Lanzhou Jiaotong University now.

**Wen-Kui Dong** received his PhD degree in 1998 from Lanzhou University, China. He is a professor in the School of Chemical and Biological Engineering at Lanzhou Jiaotong University. His current research interests are focusing on the chemistry of functional supramolecular complexes, materials and new products, as well as processes and applications of environmental chemical engineering.

**Table 1** Comparison of binding constants and detection lines between the chemosensors.

No.	sensor	Binding constant (M <sup>-1</sup> )	Detection limit (M)	Identification substance	pH range	Reference
1		$6.42 \times 10^4$	$4.7 \times 10^{-6}$	Cu <sup>2+</sup>	4~8	[63]
2		$2.4 \times 10^2$	$1.7 \times 10^{-6}$	Cu <sup>2+</sup>	4~12	[64]
3		$2.6 \times 10^4$	$3.4 \times 10^{-7}$	Al <sup>3+</sup>	4.5~9.5	[68]
4		$4.95 \times 10^4$	$8.65 \times 10^{-8}$	Al <sup>3+</sup>	5~8	[69]
5		$3.5 \times 10^{10}$	$6.62 \times 10^{-7}$	Cu <sup>2+</sup>	3~11	This work
		$3.05 \times 10^{11}$	$5.33 \times 10^{-7}$	Al <sup>3+</sup>	5~8	This work

**Scheme 1.** Synthetic route to sensor **H<sub>2</sub>L<sub>5</sub>****Scheme 1**

**Figure 1** Fluorescence spectra of chemical sensor **H<sub>2</sub>Ls** and metal ions (20 equiv.) in DMF/H<sub>2</sub>O buffer solution (**H<sub>2</sub>Ls**,  $1 \times 10^{-3}$  mol/L; Tris-HCl buffer solution, 9/1, v/v, pH = 7.20).

**Figure 2** The sensor **H<sub>2</sub>Ls** ( $1 \times 10^{-3}$  mol/L) in DMF/H<sub>2</sub>O buffer solution buffer solution for Cu<sup>2+</sup> recognition anti-interference experiment. (Emission peak at 388 nm, the black bar is the fluorescence intensity of the chemical sensor **H<sub>2</sub>Ls**, the red bar is the fluorescence intensity of the sensor **H<sub>2</sub>Ls** with Cu<sup>2+</sup> added, the blue bar is the fluorescence intensity of **H<sub>2</sub>Ls**+Cu<sup>2+</sup> after adding common metal ion. **H<sub>2</sub>Ls**,  $1 \times 10^{-3}$  mol/L; Tris-HCl buffer solution, 9/1, v/v, pH = 7.20).

**Figure 3** Proposed recognition mechanism of Cu<sup>2+</sup> by fluorescence chemical sensor **H<sub>2</sub>Ls**

**Figure 4** The photos of chemical sensor **H<sub>2</sub>Ls** using test paper (a) **H<sub>2</sub>Ls**; (b) **Lc**; (c) **Lc**+Al<sup>3+</sup>; (d) **H<sub>2</sub>Ls**+other metal ions; (e) **Lc** + other metal ions; (e) **Lc** + other metal ions+Al<sup>3+</sup> ( all taken under 365 nm ultraviolet lamp).

**Figure 5** Proposed recognition mechanism of Al<sup>3+</sup> by fluorescent chemical sensor **Lc**.

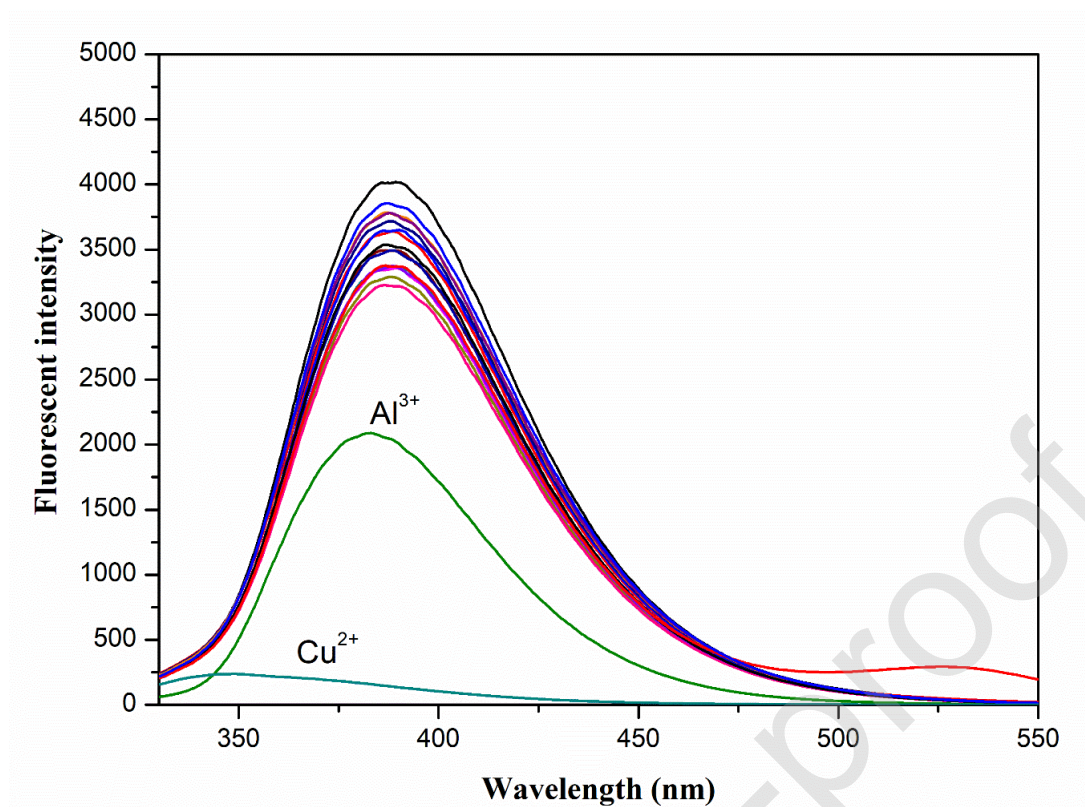


Figure 1

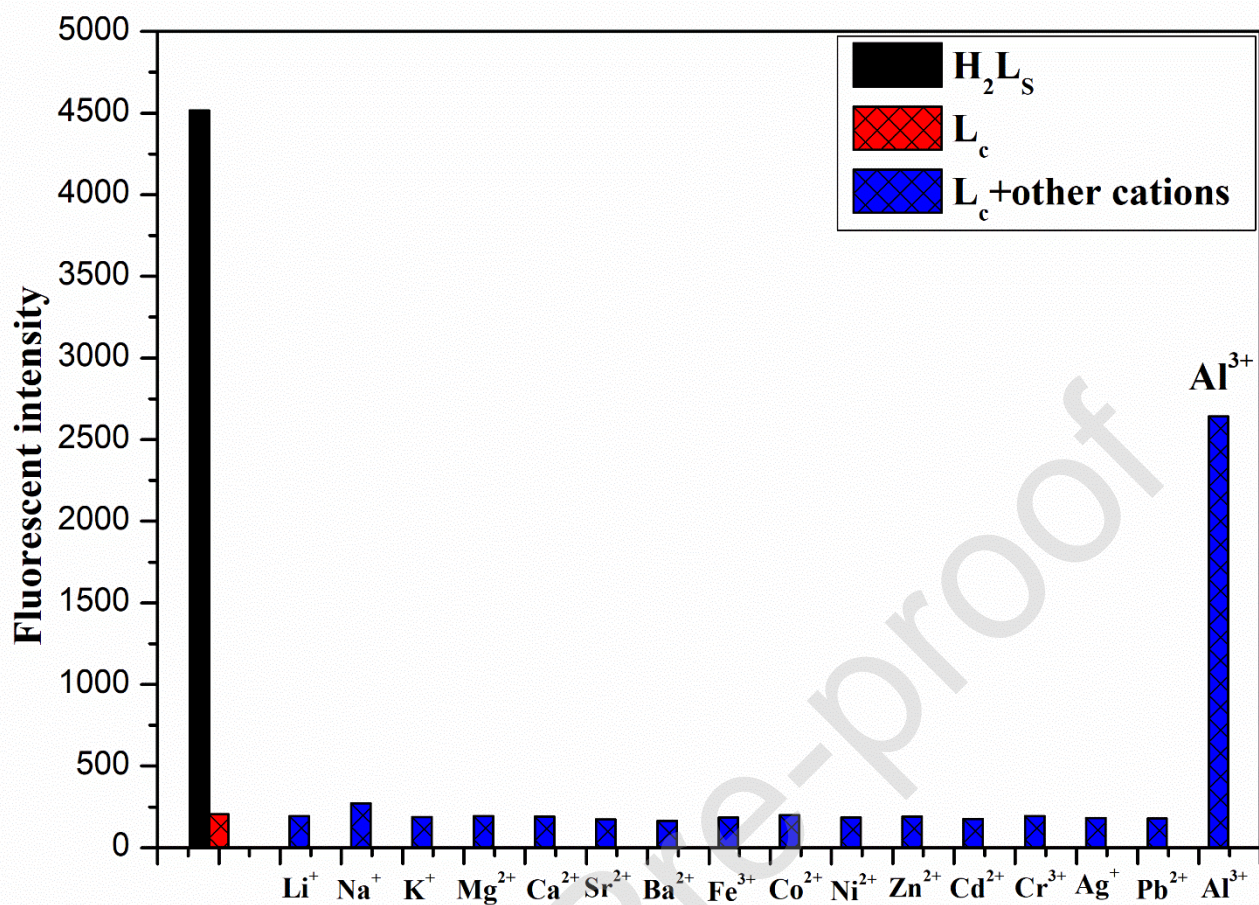


Figure 2

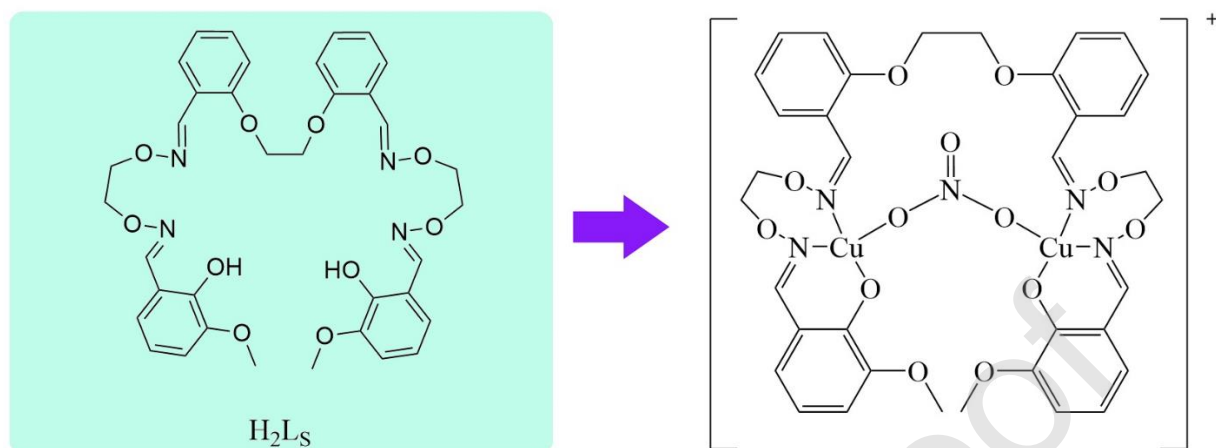
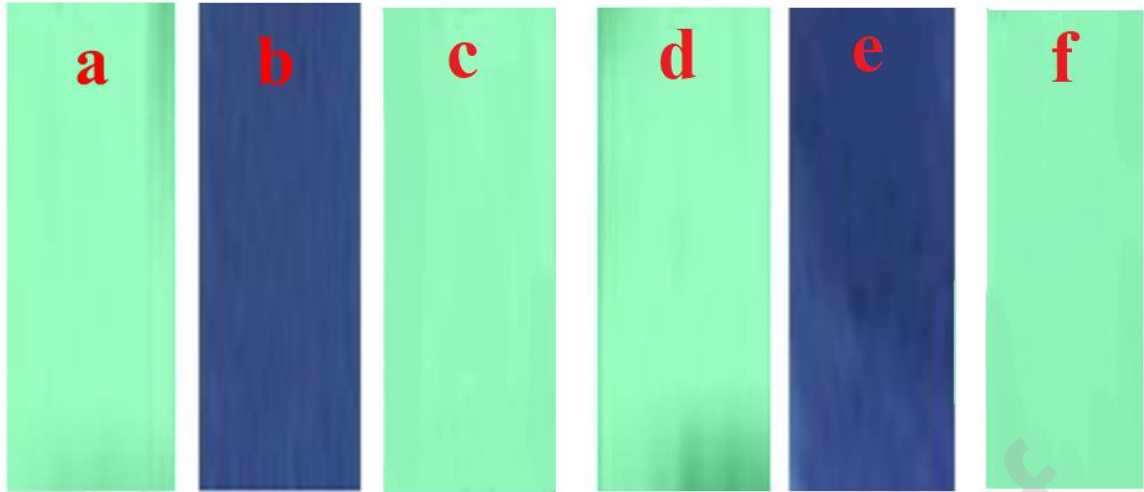


Figure 3



**Figure 4**

Journal Pre-proof

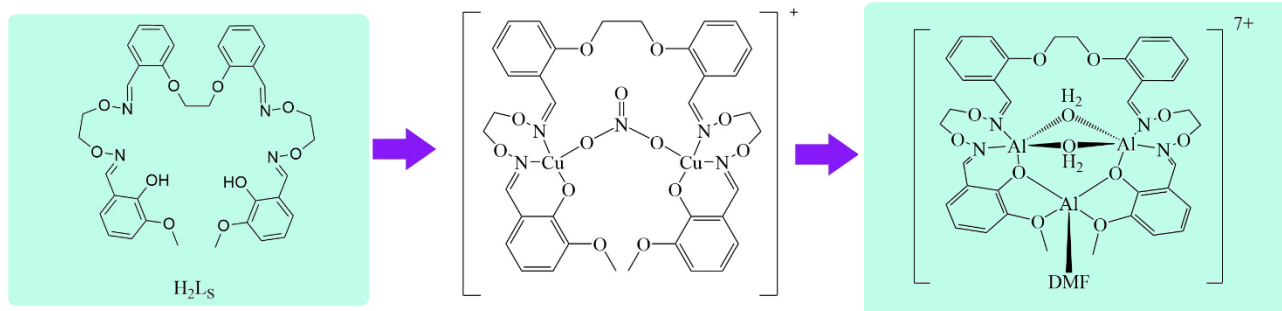


Figure 5